RSC Advances

ROYAL SOCIETY OF CHEMISTRY

www.rsc.org/advances

Whey protein isolate/gum arabic intramolecular soluble complexes improving the physical and oxidative stabilities of conjugated linoleic acid emulsions

Xiaolin Yao [a, b], Shengping Xiang [a], Ke Nie [a], Zhiming Gao [a, b], Weiqi Zhang [a], Yapeng Fang [a, b, *], Katsuyoshi Nishinari [a, b], Glyn O. Phillips [a], Fatang Jiang [a]

[a] Glyn O. Phillips Hydrocolloid Research Centre, School of Food and Pharmaceutical Engineering, Faculty of Light Industry, Hubei University of Technology, Wuhan 430068, China.

[b] Hubei Collaborative Innovation Centre for Industrial Fermentation, Hubei University of Technology, Wuhan 430068, China.

* To whom correspondence should be addressed. Tel: +86 (0) 27-88015996; Fax: +86 (0)27-88015996; Email: fangypphrc@163.com.

Abstract

Protein/polysaccharide electrostatic complexes have been widely used in food products to confer structure and stability. Intramolecular soluble complexes (ISCs) have superior emulsifying properties in stabilizing oil-in-water (o/w) emulsions. This paper investigated the potential application of ISCs stabilizing polyunsaturated fatty acids that were difficult to disperse and liable to oxidation. The idea was demonstrated using whey protein isolate/gum arabic (WPI/GA) ISCs and conjugated linoleic acid (CLA). Zeta potential measurements indicated a stoichiometry of r = 1.0 for the electrostatic complexation of WPI/GA. Excess in GA (r < 1.0) ensured the formation of stable ISCs in a specific pH range, e.g. pH 4.0-5.4 at r = 0.5. The nano-sized ISCs significantly improved the physical and oxidative stabilities of CLA emulsions in comparison with individual WPI or GA. Optimal stabilization was found at a WPI/GA concentration of 2.0 wt% for emulsions with CLA = 15 wt%. NaCl tended to dissociate ISCs when NaCl > 20 mM and therefore seriously reduced the stability of ISCs-stabilized CLA emulsions. The superiority of ISCs in stabilizing polyunsaturated fatty acids is due to the cooperative adsorption of protein and polysaccharide at emulsion interface, providing strong steric and electrostatic effects against droplet aggregation and coalescence and thus excellent physical stability. The improved oxidative stability should arise from the free radical scavenging ability of protein at emulsion interface, reducing lipid oxidation.

Keywords

Conjugated linoleic acid; Emulsion; Stability; Oxidation; Protein/polysaccharide complex

Introduction

Polyunsaturated fatty acids (PUFAs), e.g. conjugated linoleic acid (CLA; C18:2), has been demonstrated to possess numerous health benefits, including sustaining infant development, supporting cardiovascular health, cancer prevention, weight control and immunomodulation.[1] Many PUFAs are essential because they cannot be synthesized by humans and thus must be derived from the diet.[1] PUFAs are often incorporated into food products in the form of oil-in-water (o/w) emulsions due to their low water dispersibility and high sensitivity to oxidation. Oxidation of PUFAs in food matrices was accelerated by the presence of oxygen, heat, light, enzymes,

metals, and metalloproteins etc., and could cause the development of off-flavors, change in color, loss of other nutrients, and the formation of potentially toxic compounds.[2] Physically and chemically stabilizing PUFAs still proves to be a challenge in the food industry with regards to the development of PUFAs fortified functional foods.

Protein/polysaccharide combinations have been widely used in food products to confer structure and stability. Non-covalent electrostatic complexes formed by charged protein and polysaccharide attract much interest due to their important biological implications and ease to use in product formulation.[3] For example, electrostatic complexation between gelatin and pectin was used to create hydrogel particles with similar dimensions and functional attributes as starch granules for formulation of low-calorie and low-starch foods.[4] Bosnea et al. applied protein/polysaccharide electrostatic complexation as a novel microencapsulation technique to improve the viability of probiotics under different stresses.[5] Selective complexation of proteins with polysaccharide was employed as an effective tool to enrich and purify proteins.[6] Due to the combined advantages of hydrophilic polysaccharide and hydrophobic protein, protein/polysaccharide electrostatic complexes emerged as novel and unique emulsifier and foaming agent, exhibiting excellent interfacial properties. [7, 8]

Protein/polysaccharide electrostatic complexation has been well characterized by using complementary techniques including turbidimetry, light scattering, zeta potentiometers, spectroscopy and light microscopy, etc..[9, 10] The process involved the formation of soluble complexes and subsequently insoluble complexes (liquid coacervation or solid precipitate).[11, 12] In a previous study, we studied the structural transition of protein/polysaccharide electrostatic complexation in bovine serum albumin/sugar beet pectin system, and proposed a detailed phase diagram.[10] A particular phase region, i.e., intramolecular soluble complexes (ISCs), was found to behave superbly in stabilizing o/w emulsions via cooperative adsorption.[7]

The present work aimed to evaluate the potential of protein/polysaccharide ISCs in stabilizing PUFAs-based emulsions. The approach is demonstrated by using whey protein isolate (WPI)/gum arabic (GA) and CLA as a model system. GA is an anionic heterogeneous polysaccharide with branched structure. It contains a small amount of proteinaceous material that is covalently attached to the polysaccharide.[13, 14] WPI is mainly composed of β-lactoglobulin (β-lg) and α-lactalbumin.[15]

It can inhibit the oxidative deterioration of limonene in o/w emulsions due to its ability to scavenge free radical and chelate prooxidative metals.[16] Both GA and WPI exhibit surface activities and are used in the food industry as emulsifiers.[17, 18] In the work, the electrostatic complexation between WPI/GA was characterized and the experimental conditions to produce ISCs identified. The ISCs were then used to stabilize CLA emulsions, and their physical and chemical stabilities were evaluated by acceleration test and oxygen consumption measurements. The results were compared with those obtained with individual protein or polysaccharide to reveal the superiority of ISCs in stabilizing PUFAs emulsions. The results obtained in the present study are expected to shed lights on the protection of other PUFAs.

Materials and methods

Materials

GA in spray-dried form with a purity of > 94.6 % was supplied by San Ei Gen F.F.I. Inc., Japan. WPI with a purity of > 95.0 % was obtained from Davisco, USA. The biopolymers were used without further purification. Food grade CLA (C18: 2) with the principal isomer form of *cis*-9,*trans*-11 was purchased from Beijing Health Science and Technology Co. Ltd., China. The purity of CLA was 80 %. The remaining components contained 12.5 % of oleic acid, and palmitic acid, stearic acid, and linoleic acid accounted for the rest, which were measured by a gas chromatograph (Varian 3900, USA). Glucono-δ-lactone (GDL) with a purity of 99.0 % was purchased from Sigma, USA. All other chemicals used in the study were of analytical grade. Millipore water was used for the preparation of solutions.

Characterization of WPI/GA electrostatic complexes

Solution preparation

WPI and GA aqueous solutions at a concentration of 0.3 wt% were prepared by dispersing weighed amount of samples into Millipore water, followed by hydration at 25 °C during overnight on a roller mixer (30 rpm). The solutions were then mixed at different proportions to give different WPI/GA weight ratios (r = 10, 4, 2, 1, 0.5, 0.25, 0.1).

Zeta potential measurements

The zeta potential (ζ) of WPI/GA mixed solutions as a function of pH was measured at 25 °C on a Zetasizer Nano-ZS apparatus (Malvern Instruments, UK), equipped with an MPT-2 pH autotitrator. The apparatus has a 4 mW He/Ne laser emitting at 633 nm. Samples that were titrated to different pHs were circulated into a standard capillary electrophoresis cell. ζ was obtained by measuring the electrophoretic mobility U_E of charged particles using laser Doppler velocimetry at a scattering angle of 17°. ζ was linked to U_E according to the following Henry equation:[10]

$$\zeta = \frac{3\eta U_E}{2\varepsilon f(Ka)} \quad (1)$$

where ε is the dielectric constant and η the viscosity of medium. $f(Ka)$ is the Henry function which possesses a value of 1.5 under the Smoluchowski approximation.

Structural transition induced by in situ acidification

The structural transition of WPI/GA during in situ acidification using glucono-δ-lactone (GDL) was monitored by turbidimetry and light scattering, as reported previously.[9, 10] WPI/GA solution was initially adjusted at pH 8.5, and then mixed rapidly with 0.25% GDL powder to initialize in situ acidification. The change in pH with time was measured by an Orion 4 Star multifunctional pH meter (Thermo Scientific Corporation) at 25 °C. The pH-time curve was correlated with the following time dependence measurements of light scattering and turbidity to obtain the information on structural transitions at different pHs (see Figure S1).

Light scattering measurement was conducted at 25 ^{o}C using Zetasizer Nano-ZS apparatus (Malvern Instruments, UK). The average scattered light intensity at 173° (I_{173}) and intensity autocorrelation function during in situ acidification were recorded every 30 s for 150 mins. Z-averaged diffusion coefficient (D_z), obtained from the analysis of autocorrelation function,[19] was used to calculate z-averaged hydrodynamic diameter (D_h) of particles through the Stokes-Einstein equation:[11]

$$D_z = \frac{k_B T}{3\pi\eta D_h} \quad (2)$$

where η is the solvent viscosity and $k_B T$ is the thermal energy.

Turbidity measurement was performed on a UV/visible spectrophotometer (TU-1900, PERSEE, China) at a wavelength of 500 nm. The change in turbidity (τ) during in situ acidification was recorded every 30 s for 150 mins at 25 ^{o}C. τ was defined as:

$$\tau = (-1/L)\ln(I_0/I_t) \quad (3)$$

where L is the optical path length, I_0 is the incident light intensity and I_t is the transmitted light intensity.

Characterization of CLA emulsions stabilized with WPI/GA complexes

Emulsion preparation

Primary emulsions were prepared by blending 15.0 wt% CLA with 85 wt% aqueous phase containing WPI/GA at different concentrations (0.1-5.0 wt%), using a high-speed blender (Polytron PT 2100) at 26,000 rpm/min for 3 mins. The primary emulsions were further homogenized by a high-pressure homogenizer (Microfluidics M-110L, USA) at 75 MPa for one pass. The homogenization was carried out in an ice bath to minimize the extent of lipid oxidation.

Particle size analysis

The long-term stability of emulsions was evaluated with acceleration test at 40 °C. The particle size distribution of emulsions was measured using a laser diffraction technique (MasterSizer 2000, Malvern Instruments, UK). The emulsions were dropwise added into the dispersing unit until a laser obscuration of 10% was achieved, and stirred continuously to avoid multiple scattering effects. The refractive index values used for disperse and continuous phases were 1.52 and 1.33, respectively. An absorption coefficient of 0.01 was used for all the samples. The droplet diameters of the emulsions were determined as D[3,2] and D[4,3], representing the surface-weighted and volume-weighted mean diameters, respectively. D[4,3] was particularly used to monitor the stability of the emulsions during storage, as it is more sensitive to the development of large droplets. All the measurements were conducted in triplicate and average values were reported.

Based on D[3,2], the specific surface area (S_v) of emulsions was calculated according to the

following equations:

$$S_v = 6\varphi/\mathrm{D}[3,2]\ (\mathrm{m}^2/\mathrm{mL\ emulsion}) \quad (4)$$

$$\varphi = (\rho_{\mathrm{aq}} - \rho_{\mathrm{em}})/(\rho_{\mathrm{aq}} - \rho_{\mathrm{oil}}) \quad (5)$$

where φ represents the volume fraction of dispersed phase, and ρ_{aq}, $\rho_{oil,}$ and ρ_{em} are the densities of the aqueous phase, oil phase and the whole emulsion, respectively.[20]

Confocal laser scanning microscopy

The microstructure of emulsions was imaged by a Zeiss LSM 510 META (Carl Zeiss AG, Germany) inverted confocal laser scanning microscope (CLSM), equipped with a helium neon laser (He/Ne) emitting at 547 nm. About 1 mL of emulsion was stained with 40 μL of 0.02 wt % rhodamine B, which results in emulsion droplets appearing as bright regions. A small drop of the sample was loaded onto a slide glass for visualization at 25 °C.[21]

Oxidative stability analysis

The oxidative stability of emulsions was evaluated by oxygen consumption measurements,[22] using a Clark-type oxygen electrode (Chlorolab 2, Hansatech Instruments Ltd., UK). The temperature was controlled at 40 °C by a Poly stat refrigerated bath (Cole-Parmer Instrument Co., Vernon Hills, IL, USA) and the illumination was provided by a light housing and a stabilized power supply (LS2, Hansatech Instruments, UK). Emulsions were bubbled with air (about 3 min) to achieve a saturation of oxygen before measurements. 2mL of the emulsions was transferred into the oxygen electrode chamber and was constantly agitated with a magnetic stirrer. The changes in oxygen concentration were monitored for 4 mins, and the oxygen consumption rate was read from the linear slope of oxygen concentration against time. All the measurements were repeated independently in triplicate and average results with standard deviations were reported. The statistics analysis was performed with ANOVA carried out by SPSS 19.0.

Results and Discussion

Electrostatic complexation of WPI/GA

Stoichiometry of WPI/GA complexation

Figure 1A displays ζ values of WPI/GA mixtures at varying protein/polysaccharide ratios (r) as a function of pH. The total concentration of biopolymers was 0.3%. The isoelectric point (IEP) of pure WPI was 4.8, which is close to the values reported in the literature.[11] Pure GA attained a saturated ζ value of -25 mV at pHs above 5.0, and approached to zero when the pH was lowered to 2.0 due to the protonation of carboxylic groups around their pKa value.[9, 10] Decreasing r resulted in a shift of ζ profiles to lower pHs and therefore a lower IEP for WPI/GA mixtures. Figure 1B is the plot of IEP against r. A sigmoid transition of IEP was observed around r = 1.0, which indicated the maximum stoichiometry of WPI/GA.[10] When r > 1.0, the possible binding sites of GA were fully occupied by excessive WPI molecules. When r < 1.0, GA was in excess and the free carboxylic groups (un-occupied binding sites) dominated the IEP via the mechanism of protonation. The complexes formed had a negative ζ, which was high enough to stabilize the complexes formed.[10]

Formation of intramolecular soluble complexes

Our previous studies revealed that ISCs between charged protein and polysaccharide could form within a specific pH range when the polysaccharide was in excess. Here, the identification of these ISCs was exemplified for WPI/GA at r = 0.5. Figure 2A illustrates the complexation of 0.3 wt% WPI/GA aqueous mixture with 10mM NaCl at r = 0.5, as monitored by light scattering and turbidimetry. With lowering pH, both I_{173} and τ exhibited a slight increase around pH = 5.4, while D_h remained nearly unchanged. This pH value was defined as pH_o, which was considerably higher than the IEP of WPI. Although WPI was overall negatively charged at pHs > IEP, the positive patches presented at the protein surface, as suggested previously,[9, 10] could have electrostatically interacted with the negatively charged GA molecules. The hydrophobic aggregation of WPI molecules when pH approached to its IEP could also contribute to the slight increase in I_{173} and τ.[7, 8] After a plateau region, I_{173}, τ and D_h increased dramatically when pH was lower than 4.0. This characteristic pH was defined as pH_c, and had been considered as an indication of the formation of intermolecular complexes. The pH range in between 4.0 and 5.4 was assigned to the formation of ISCs, according to the state diagram proposed previously.[10] Under this specific condition, the binding of WPI to GA happened within individual GA molecules, and no bridging between GA molecules is believed to occur. ISCs represent a rather stable state of the electrostatic

complexation of WPI/GA, as manifested by the plateaus in I_{173} and $\tau.D_h$ also attained a nearly constant value of ~ 50 nm within this specific pH range (see Figure S2).

Figure 2B shows the influence of ionic strength on the formation of ISCs. When NaCl ≤ 20 mM, pH_o and pH_c was nearly independent of ionic strength. It suggests that the electrostatic complexation between WPI and GA is insensitive to the addition of NaCl at lower ionic strength. With increasing concentration of NaCl, pH_o and pH_c started to decrease considerably when NaCl > 20 mM. With further increasing NaCl above 60 mM, the transitions associated with pH_o and pH_c nearly disappeared (data not shown). This indicated that the ISCs started to be unstable when NaCl > 20 mM and was nearly dissociated completely when NaCl > 60 mM. Similar effects of ionic strength was observed for the electrostatic complexation of bovine serum albumin/sugar beet pectin and gelatin/κ-carrageenan systems.[10, 23] It was generally believed that ionic strength reduced protein/polysaccharide complexation by exerting an electrostatic screening effect.[11] The microions presented in the solution screened the charges of the polymers and thus reduced the range of their associative interactions.

Physical stability of CLA emulsions stabilized with ISCs

Effect of ISCs concentration

The capability of ISCs to stabilize CLA based o/w emulsions was evaluated by using WPI/GA ISCs formed at r = 0.5 and pH = 4.4. Figure 3A shows the change of D[4,3] for freshly prepared 15% CLA emulsions, as a function of the concentration of ISCs. It exhibited an interesting U-shape variation. At lower ISCs concentrations, i.e., < 1.0 wt%, D[4,3] was reduced with increasing the emulsifier concentration. This should be attributed to an increased surface coverage of CLA emulsion droplets by the adsorption of ISCs. When 1.0 wt% < ISCs < 3.0 wt%, D[4,3] tended to level off and attains a minimum value at ISCs = 2.0 wt%. This indicated an optimal concentration range of ISCs in stabilizing CLA emulsions, where a full surface coverage of emulsion droplets had been achieved.[24] When the ISCs concentration increased above 3.0 wt%, D[4,3] turned to increase again. The increase in D[4,3] at higher ISCs concentrations cannot be explained explicitly at this stage. A similar phenomenon had been observed in GA-stabilized CLA emulsions where the excess of GA led to a reduced stability of CLA emulsions.[22] A tentative

explanation could be that the excessive concentration of free emulsifiers in the aqueous phase increased the depletion interaction between emulsion droplets, promoting instabilities such as flocculation, aggregation, coalescence, and creaming.[25, 26]

Figure 3B shows the particle size distribution of CLA emulsions at typical concentrations of WPI/GA ISCs. The emulsions at ISCs = 0.5 and 2.0 wt% both had a relatively monomodal distribution, while the emulsion at ISCs = 5.0% showed a bimodal distribution. Among the three ISCs concentrations, ISCs = 2.0 wt% yielded the smallest droplet size. The micrographs taken at the typical ISCs concentration, shown as insets in Figure 3A, supported the results of particle size measurements. The microstructures of the emulsions at ISCs = 0.5 and 5.0 wt% exhibited a stronger tendency of aggregation. Distinctly large emulsion droplets could be observed at ISCs = 0.5 wt%. In contrast, the emulsion at ISCs = 2.0 wt% was well dispersed with relatively fine particles.

In brief summary, the potential conditions enabling production of fine CLA emulsions were 1.0 wt% < ISCs < 3.0 wt%, with an optimal concentration at 2.0 wt%. Further tests on the stability of the emulsions prepared under these conditions were carried out. Figure 4 shows the volume weighted diameter D[4,3] as a function of storage time during acceleration test at 40 ^{o}C. In the concentration range of 1.0 wt% < ISCs < 3.0 wt%, the emulsions had rather good stability, with D[4,3] almost constant for 7 days during acceleration at 40 ^{o}C. When ISCs fell out of this particular concentration range, i.e., ISCs < 1.0 wt% or ISCs > 3.0 wt%, the emulsions showed considerable growth in D[4,3]. The instability could be due to the aggregation tendency that was augmented during acceleration test. The bulk appearance of the emulsions at the typical ISCs concentrations during acceleration test at 40 ^{o}C is shown in Figure 4B. At 0.5 wt% ISCs, a creaming layer was observed on the 3rd day of storage, and its boundary moved up on the 7th day. This indicated an increased extent of creaming or phase separation. The emulsion with 5.0 wt% ISCs also exhibited significant creaming on the 3rd and 7th days of storage. In comparison, the emulsion with 2.0 wt% ISCs remained homogenous throughout the storage, without discernible creaming/phase separation. The results above showed that the WPI/GA ISCs could yield the best physical stability of CLA emulsions in an optimal concentration range of 1.0 wt% < ISCs < 3.0 wt%.

Comparison with individual WPI and GA

The emulsifying performance of WPI/GA ISCs was compared with those of individual protein and polysaccharide. The emulsion contained 15 wt% CLA as the oil phase and 2.0 wt% WPI/GA ISCs (r = 0.5, pH = 4.4) as the emulsifier. Equivalent amounts of WPI (0.67 wt%) or GA (1.33 wt%) were used for comparison (Figure 5). The particle size distribution of the emulsion with 1.33 wt% GA showed an average droplet size of D[4,3] ≈ 3.2 μm, which was significantly larger than that of ~ 0.67 μm for 2.0 wt% WPI/GA ISCs. In a previous study, we demonstrated that the optimal concentration of GA to stabilize CLA emulsion was 5.0 wt%, which yielded D[4,3] ≈ 1.0 μm.[22] Even at this optimal concentration, GA could not match the emulsifying performance of WPI/GA ISCs. The emulsion with 0.67 wt% WPI showed a broad bimodal distribution, with D[4,3] as large as ~ 80.6 μm. The poor emulsifying performance should be attributed to the loss of solubility when pH was close to the IEP of WPI.[7] Charge neutralization around the isoelectric point decreased the electrostatic stabilization and could also explain the poor emulsifying performance. The comparison here suggested that the ISCs had superior emulsifying performance over individual protein or polysaccharide in stabilizing CLA emulsions. The finer emulsion droplets obtained with ISCS could possibly mean a faster/more complete digestion process and an improved bioavailability for CLA when it is incorporated into oil-in-water emulsion, as the specific surface area of emulsion increases with decreasing droplet size.[27] The increase in specific surface area was generally believed to a benefiting factor for digestion and cell uptake.

The stabilities of the emulsions with WPI, GA and ISCs against acceleration test are presented in Figure 6A. D[4,3] of the ISCs-stabilized emulsion showed negligible change during 7-day storage at 40 ^{o}C, indicating a fairly stable emulsion. The D[4,3] of the GA-stabilized emulsion was larger than that of ISCs-stabilized emulsion, and increased slightly during the storage. However, the D[4,3] of the WPI-stabilized emulsion grew dramatically during the storage, indicating a poor stability. The macroscopic observations in Figure 6B show clear phase separations in the emulsions stabilized with WPI and GA, while there is no sign of any phase separation in the emulsion stabilized with ISCs. The acceleration tests suggested an increased physical stability of CLA emulsions with ISCs > GA > WPI. The superiority of ISCs in stabilizing CLA emulsion was due to the cooperative adsorption of WPI and GA at the oil-water interface, providing strong steric

and electrostatic effects against droplet aggregation and coalescence and thus improved physical stability.[7]

Effect of ionic strength

The effect of ionic strength on the physical stability of ISCs-stabilized CLA emulsion was investigated. The change of D[4,3] as a function of NaCl concentration is plotted in Figure 7, for emulsions before and after storage at 40 °C for 7 days. When NaCl < 20mM, no significant change in D[4,3] could be observed. Once NaCl concentration increased above 20 mM, D[4,3] started to increase markedly. Moreover, the extent of increase was higher after 7-day storage, compared with that before storage. This indicated a deterioration of the physical stability of CLA emulsion. It was attributing to the electrostatic screening effect of NaCl on the formation of ISCs.

Oxidative stability of CLA emulsions stabilized with ISCs

The oxidative stability of CLA emulsions stabilized with ISCs, WPI or GA alone was evaluated. Oxygen consumption rate (R) was calculated from the slopes of oxygen concentration-time curves. R/S_v represented the oxygen consumption rate per unit area of the emulsion droplet surface, and thus normalized the effect arising from the difference in emulsion droplet size distributions.[28] R/S_v was linked to CLA oxidation that consumed oxygen to form lipid peroxyl radicals, according to the oxidation mechanism reported previously.[22] Figure 8 compares R/S_v for CLA emulsions stabilized with ISCs at different concentrations at 40 °C with or without exposure to light. The R/S_v for emulsion exposed to light was higher than that without exposure to light. It demonstrated that light might promoted lipid oxidation, but the effect was not significant ($P > 0.05$). The lowest R/S_v was found for emulsions with 2.0 wt% ISCs at both conditions. It was inferred that the oxidation of CLA emulsions was minimal at 2.0 wt% ISCs. The optimal concentration for oxidative stability was the same with that for physical stability (Figure 3A). Moreover, compared with individual WPI (0.67 wt%) and GA (1.33 wt%), the emulsions stabilized with 2.0 wt% ISCs showed a significant lower R/S_v ($P < 0.05$) (Figure 9), indicating the superiority of ISCs in preventing polyunsaturated fatty acid-based emulsions from being oxidized.

In a previous study,[22] we made a supposition that a physically stable emulsion was a prerequisite for the chemical stability of CLA, which also applied to the ISCs. The cooperative

adsorption of WPI/GA ISCs onto the oil-water interface formed a thick and compact interfacial layer around CLA emulsion droplets, leading to an improved emulsifying functionality and stability. The interface could provide a strong steric and electrostatic stabilization effects against the aggregation and coalescence of emulsion droplets. On the other hand, CLA oxidation was highly dependent on the interaction between lipid hydroperoxides at emulsions droplet interface and transition metals present in the aqueous phase.[29, 30] The thick and compact interface layer could act as a physical barrier to the metals, isolating them from lipid hydroperoxides and thus preventing the formation of free radicals to attack CLA.

It should be pointed out that although the emulsion with 0.5 wt% ISCs was much finer and stable than that with 5 wt% ISCs (Figures 3 and 4), the two emulsions showed more or less the same value of R/S_v. This could be explained by the presence of excessive ISCs and hence protein in the emulsion with 5.0 wt% ISCs. It is well known that proteins have ability to chelate metal ions and to scavenge free radicals, reducing lipid oxidation.[31-35] CLA was reported to be efficiently protected from oxidative attack by complexation with amino acids (lysine or arginine), mainly attributed to the antioxidant effect of the amino acids through scavenging the oxygen radicals.[36] The higher amount of protein in the emulsion with 5.0 wt% ISCs might counteract the increased lipid oxidation resulting from its poor physical stability. Similar effects had been observed in β-lg stabilized emulsions.[37, 38] The oxygen uptake in the β-lg stabilized emulsion with excessive β-lg was much lower, due to the antioxidant effect of the non-adsorbed β-lg. The antioxidant mechanisms of protein were thought to be dependent on protein tertiary structure. In order for a protein to chelate aqueous metals, the amino acid residues responsible for metal binding must be sufficiently exposed.[39, 40] However, protein oxidation could lead to the formation of carbonyls, intra- and intermolecular cross-linking through the formation of disulphide bonds and dityrosine, a decrease in protein solubility, and the fragmentation of peptide backbone.[41] The negative impact of protein oxidation appeared to have limited effect on the physicochemical stabilities of the CLA emulsions.

Conclusion

This paper evaluated the potential of the WPI/GA ISCs in stabilizing PUFAs-based emulsions.

The results showed that the nano-sized ISCs (~ 50 nm) could significantly improve the physicochemical stabilities of CLA emulsions in comparison with individual protein or polysaccharide. The superiority of ISCs originated from the cooperative adsorption of protein and polysaccharide on to the emulsion interfaces, providing steric and electrostatic stabilization as well as free radicals-scavenging ability. The results can guide the design of protective delivery system for polyunsaturated fatty acids based on oil-in-water emulsion technique.

Acknowledgement

We acknowledge financial support from the National Natural Science Foundation of China (31470096, 31101260, 31322043, 31501430), Projects from Hubei Provincial Department of Science and Technology (2014CFB602).

References

1 B. Chen, D. J. McClements and E. A. Decker, *Annu. Rev. Food Sci. T.*, 2013, 4, 35-56.
2 F. Shahidi and Y. Zhong, *Chem. Soc. Rev.*, 2010, 39, 4067-4079.
3 C. Schmitt and T. Sl., *Adv. Colloid Interface Sci.*, 2011, 167, 63-70.
4 B. C. Wu, B. Degner and D. J. McClements, *J. Phys.-Concens. Mat.*, 2014, 26, 464104.
5 L. A. Bosnea, T. Moschakis and C. G. Biliaderis, *Food Bioprocess Tech.*, 2014, 7, 2767-2781.
6 Y. Xu, M. Mazzawi, K. Chen, L. Sun and P. L. Dubin, *Biomacromolecules*, 2011, 12, 1512-1522.
7 X. Li, Y. Fang, S. Al-Assaf, G. O. Phillips and F. Jiang, *J. Colloid Interf. Sci.*, 2012, 388, 103-111.
8 X. Li, Y. Fang, G. O. Phillips and S. Al-Assaf, J. Agric. Food Chem., 2013, 61, 1388-1396.
9 G. Mekhloufi, C. Sanchez, D. Renard, S. Guillemin and J. Hardy, *Langmuir*, 2004, 21, 386-394.
10 X. Li, Y. Fang, S. Al-Assaf, G. O. Phillips, X. Yao, Y. Zhang, M. Zhao, K. Zhang and F. Jiang, *Langmuir*, 2012, 28, 10164-10176.
11 F. Weinbreck, R. de Vries, P. Schrooyen and C. G. de Kruif, *Biomacromolecules*, 2003, 4, 293-303.
12 F. Weinbreck, H. S. Rollema, R. H. Tromp and C. G. D. Kruif, *Langmuir*, 2004, 20, 6389-6395.
13 N. Garti and M. E. Leser, *Polym. Advan. Technol.*, 2001, 12, 123-135.
14 T. Mahendran, P. A. Williams, G. O. Phillips, S. Al-Assaf and T. C. Baldwin, *J. Agric. Food Chem.*, 2008, 56, 9269-9276.
15 A. K. Stone and M. T. Nickerson, *Food Hydrocolloids*, 2012, 27, 271-277.
16 D. Djordjevic, L. Cercaci, J. Alamed, D. J. Mcclements and E. A. Decker, *J. Food Sci.*, 2008, 73, 167-172.
17 A. Benichou, A. Aserin and N. Garti, *J. Disper. Sci. Technol.*, 2002, 23, 93-123.
18 A. Paraskevopoulou, D. Boskou and V. Kiosseoglou, *Food Chem.*, 2005, 90, 627-634.

19 F. Weinbreck, V. R. De, P. Schrooyen and C. G. de Kruif, *Biomacromolecules*, 2003, 4, 293-303.
20 R. A. Buffo, G. A. Reineccius and G. W. Oehlert, *Food Hydrocolloids*, 2001, 15, 53-66.
21 L. Wang, Y. Cao, K. Zhang, Y. Fang, K. Nishinari and G. O. Phillips, *Colloid Surf. A-Physicochem. Eng. Asp.*, 2015, 482, 604-610.
22 X. Yao, Q. Xu, D. Tian, N. Wang, Y. Fang, Z. Deng, G. O. Phillips and J. Lu, *J. Agric. Food Chem.*, 2013, 61, 4639-4645.
23 Y. Fang, L. Li, C. Inoue, L. Lundin and I. Appelqvist, *Langmuir*, 2006, 22, 9532-9537.
24 S. Xiang, X. Yao, W. Zhang, K. Zhang, Y. Fang, K. Nishinari, G. O. Phillips and F. Jiang, *Food Hydrocolloids*, 2015, 48, 110-116.
25 E. Dickinson, *Food Hydrocolloids*, 2009, 23, 1473-1482.
26 T. Moschakis, B. S. Murray and E. Dickinson, *Langmuir*, 2006, 22, 4710-4719.
27 S. Marze, *Food Funct.*, 2015, 6, 3218-3227.
28 A. Goki, K. Naoko, H. Masashi and M. Kazuo, *J. Oleo Sci.*, 2009, 58, 329-338.
29 J. R. Mancuso, D. J. Mcclements and E. A. Decker, *J. Agric. Food Chem.*, 1999, 47, 4112-4116.
30 L. Mei, D. J. Mcclements and E. A. Decker, *J. Agric. Food Chem.*, 1999, 47, 2267-2273.
31 L. L. Wang and Y. L. Xiong, *J. Agric. Food Chem.*, 2005, 53, 9186-9192.
32 F. Habibollah, M. D Julian and E. A. Decker, *J. Agric. Food Chem.*, 2004, 52, 4558-4564.
33 V. Angélique, V. Michèle, B. Isabelle, M. Nathalie and G. Claude, *J. Agric. Food Chem.*, 2005, 53, 1514-1520.
34 M. Sugiarto, A. Ye, M. W. Taylor and H. Singh, *Dairy Sci. Technol.*, 2010, 90, 87-98.
35 M. R. Clausen, L. H. Skibsted and S. Jan, *J. Agric. Food Chem.*, 2009, 57, 2912-2919.
36 S. Koohikamali, S. M. M. Kamal, *Eur. J. Lipid Sci. Technol.*, 2014, 117, 637-645.
37 C. Berton, M. H. Ropers, M. Viau and C. Genot, *J. Agric. Food Chem.,* 2011, 59, 5052-5061.
38 R. Elias, D. McClements and E. Decker, *Food Chem.*, 2007, 104, 1402-1409.
39 J. J. Baumy and G. Brule, *Dairy Sci. Technol.*, 1988, 68, 409-417.
40 M. Diaz and E. A. Decker, *J. Agric. Food Chem.*, 2004, 52, 8208-8213.
41 H. Chen, J. Diao, Y. Li, Q. Chen and B. Kong, *Meat Sci.*, 2016, 111, 60-66.

Captions for figures

Figure 1. Zeta potential ζ as a function of pH for WPI/GA mixtures with varying protein/polysaccharide ratios (*r)* (A). Plot of isoelectric point (IEP) against *r* (B). The logarithmic x-axis was broken for inclusion of the data points of pure WPI and GA (indicated in yellow). The total biopolymer concentration is 0.3 wt%.

Figure 2. Evolution of the turbidity at 500 nm (τ, □), scattered light intensity at 173° (I_{173}, ○), and hydrodynamic diameter (D_h, △) as a function of pH during GDL-induced acidification for a 0.3wt% WPI/GA mixture at r = 0.5 with 10mM NaCl (A). Effect of NaCl addition on the typical pHs (■, pHo; ▲, pHc) for the WPI/GA complex formation (B).

Figure 3. Volume-weight mean diameter D[4,3] of freshly prepared CLA emulsions as a function of the concentration of WPI/GA ISCs (A), and the particle size distribution at typical ISCs concentrations (B). The insets in Figure A represent the microstructures of CLA emulsions observed using CLSM at the typical ISCs concentrations.

Figure 4. The plot of volume weighted mean diameter D[4,3] against storage time at 40 °C for CLA emulsions prepared with various concentrations of WPI/GA ISCs (A) and the images of the emulsions taken at 0, 3 and 7 days of the storage for the emulsions with ISCs = 0.5, 2.0 and 5.0 wt% (B).

Figure 5. Particle size distributions of CLA emulsions stabilized by 0.67 wt% WPI, and 1.33 wt% GA and 2.0 wt% WPI/GA ISCs (r = 0.5) at pH 4.4.

Figure 6. The plot of volume weighted mean diameter D[4,3] against storage time at 40 °C for CLA emulsions prepared with 0.67 wt% WPI, 1.33 wt% GA and 2.0 wt% WPI/GA ISCs, respectively (A), and the corresponding images of the emulsions taken at 0, 3 and 7 days of the storage (B).

Figure 7. Plot of D[4,3] as a function of NaCl concentration before and after the storage at 40 °C for 7 days. The CLA emulsion was stabilized with 2.0 wt% WPI/GA ISCs (r = 0.5, pH=4.4).

Figure 8. Normalized oxygen consumption rate R/S_v for CLA emulsions stabilized with various ISCs concentrations at 40 °C with (dot column) and without (blank column) exposure to light. Oxygen consumption rate (R) was calculated from the slopes of oxygen concentration-time curves. S_v stands for the specific surface area of CLA emulsions. Values of each column with different superscripts (a-f) are significantly different at $P < 0.05$.

Figure 9. Normalized oxygen consumption rate R/S_v for CLA emulsions stabilized by WPI, GA, and ISCs respectively at 40 °C with (dot column) and without (blank column) exposure to light. Oxygen consumption rate (R) was calculated from the slopes of oxygen concentration-time curves. S_v stands for the specific surface area of CLA emulsions. Values of each column with different superscripts (a-d) are significantly different at $P < 0.05$.

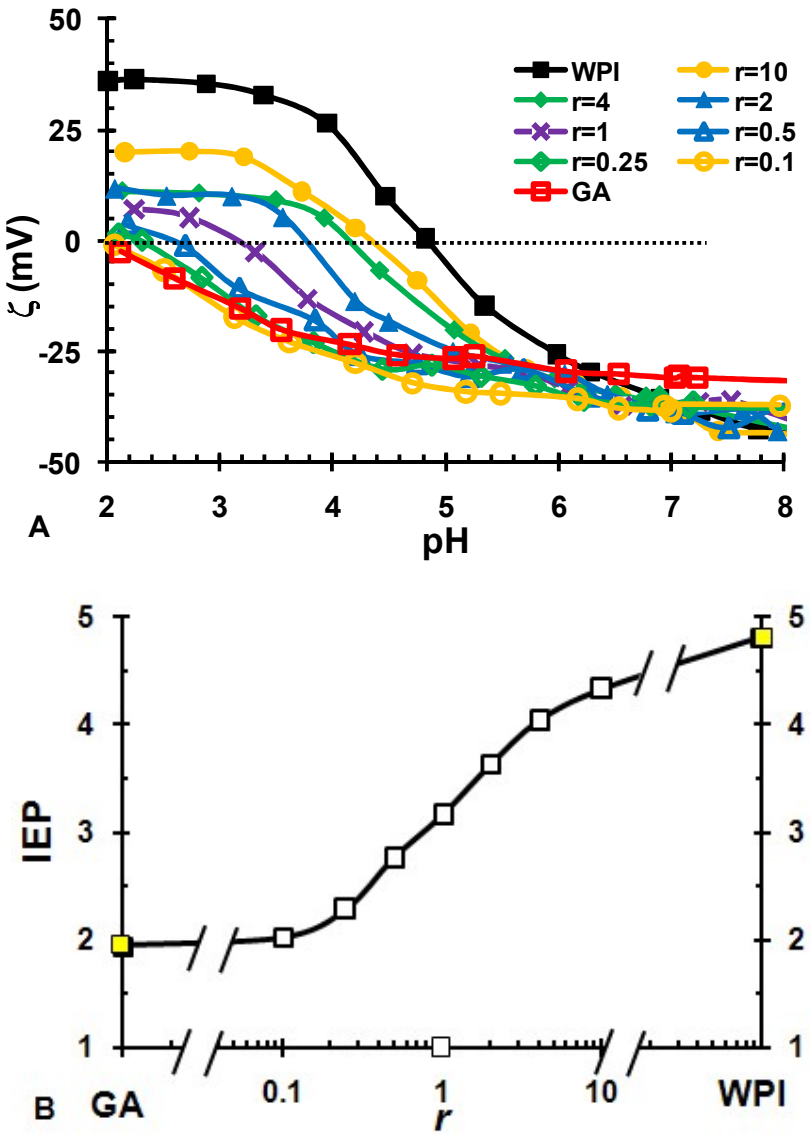

Figure 1. Zeta potential ζ as a function of pH for WPI/GA mixtures with varying protein/polysaccharide ratios (*r)* (A). Plot of isoelectric point (IEP) against *r* (B). The logarithmic x-axis was broken for inclusion of the data points of pure WPI and GA (indicated in yellow). The total biopolymer concentration is 0.3 wt%.

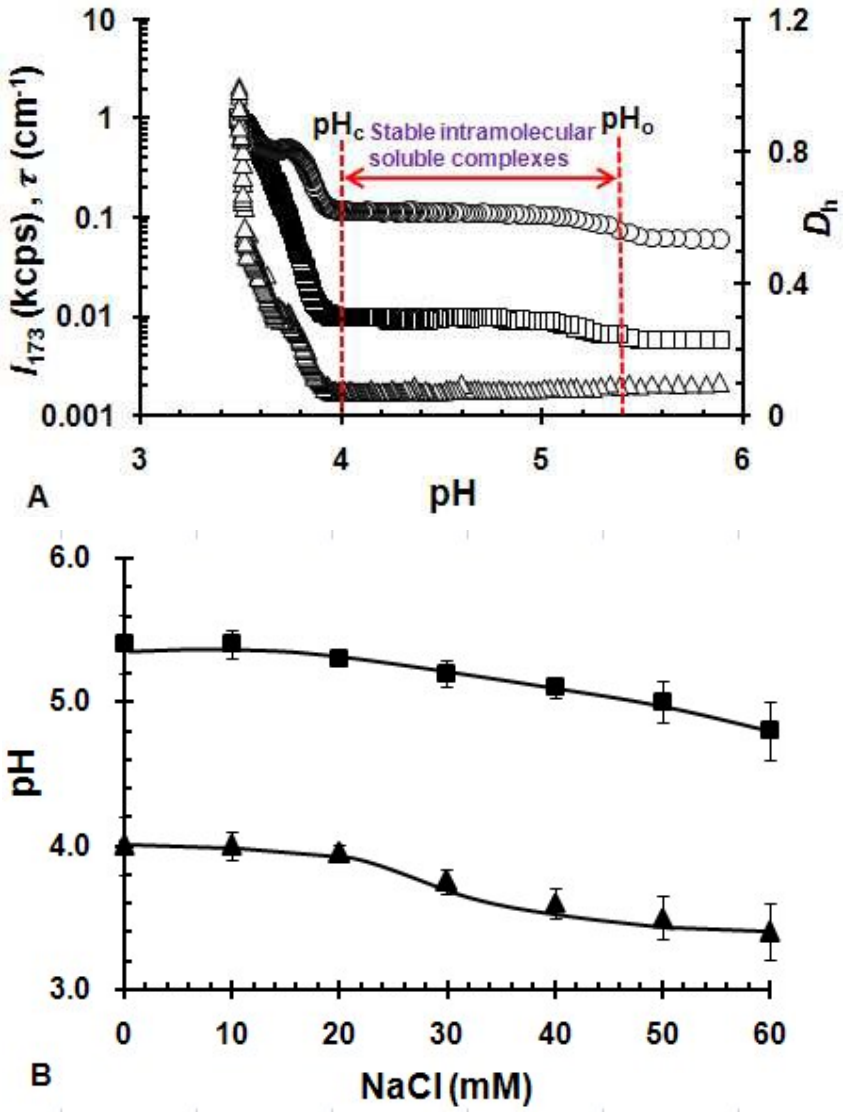

Figure 2. Evolution of the turbidity at 500 nm (τ, □), scattered light intensity at 173° (I_{173}, ○), and hydrodynamic diameter (D_h, △) as a function of pH during GDL-induced acidification for a 0.3wt% WPI/GA mixture at r = 0.5 with 10mM NaCl (A). Effect of NaCl addition on the typical pHs (■, pH$_o$; ▲, pH$_c$) for the WPI/GA complex formation (B).

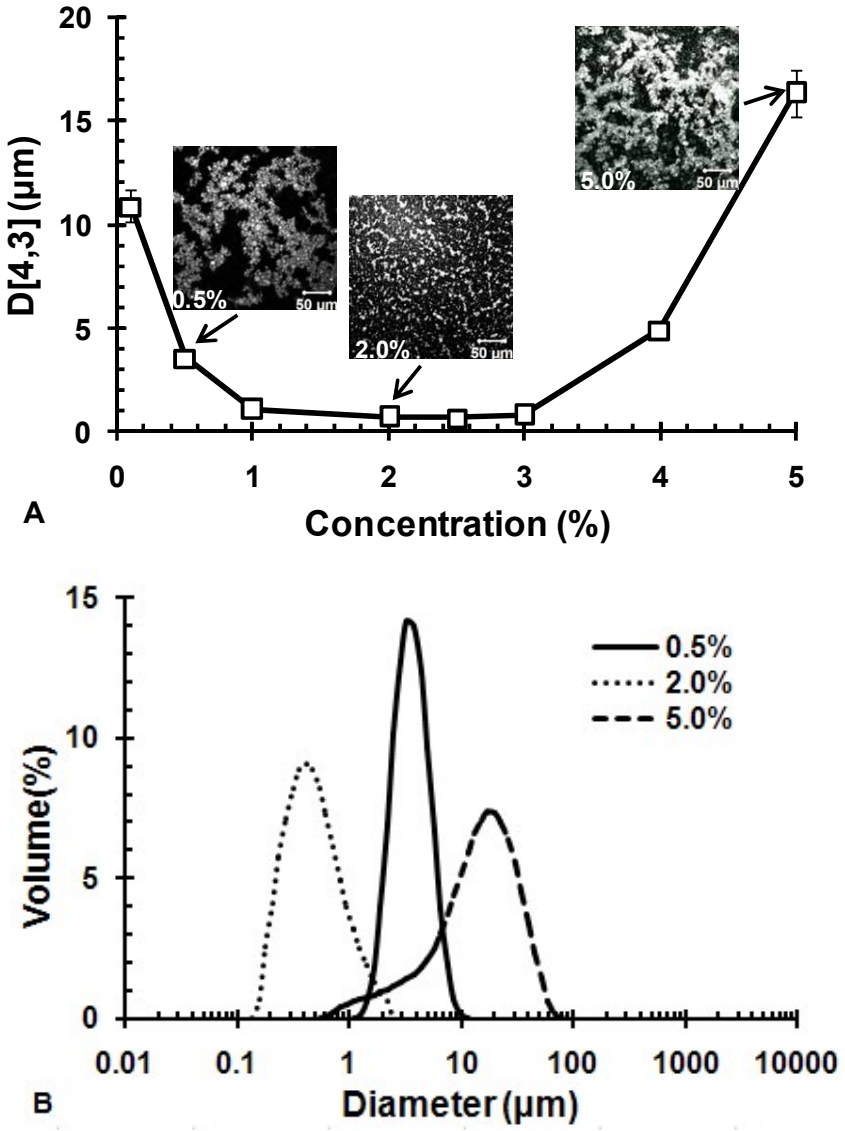

Figure 3. Volume-weight mean diameter D[4,3] of freshly prepared CLA emulsions as a function of the concentration of WPI/GA ISCs (A), and the particle size distribution at typical ISCs concentrations (B). The inlets in Figure A represent the microstructures of CLA emulsions observed using CLSM at the typical ISCs concentrations.

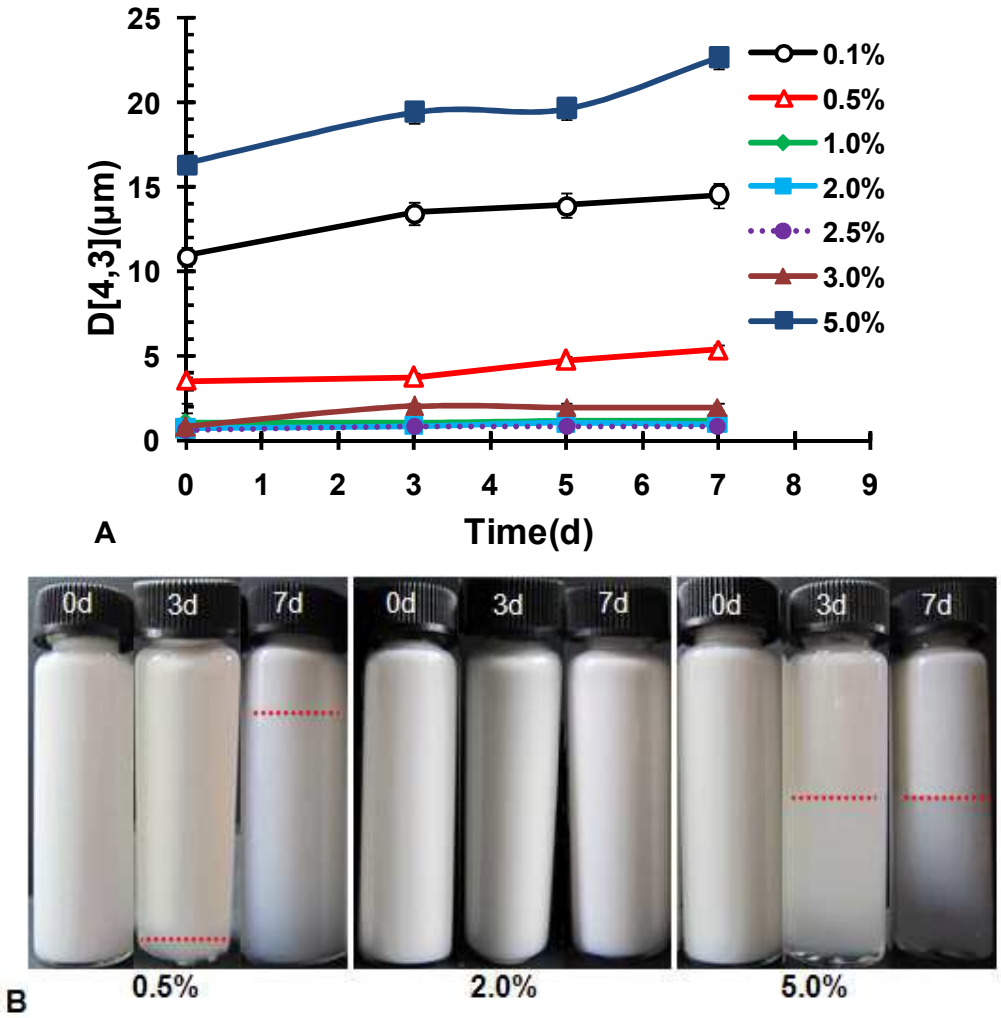

Figure 4. The plot of volume weighted mean diameter D[4,3] against storage time at 40 °C for CLA emulsions prepared with various concentrations of WPI/GA ISCs (A) and the images of the emulsions taken at 0, 3 and 7 days of the storage for the emulsions with ISCs = 0.5, 2.0 and 5.0 wt% (B).

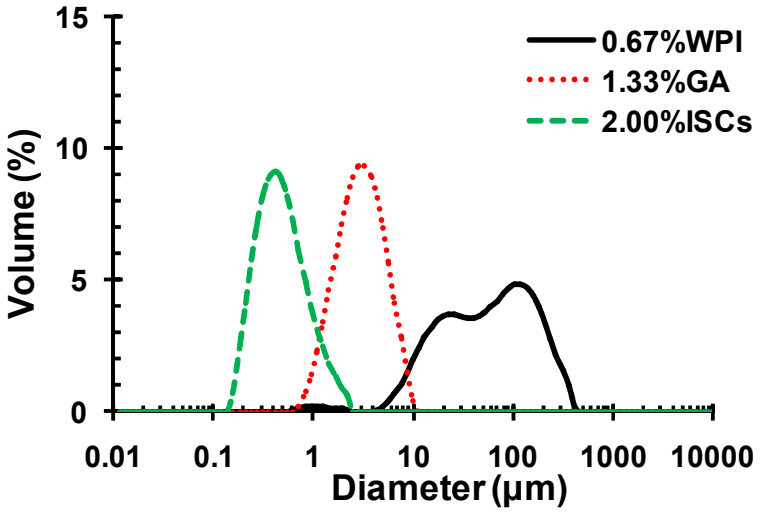

Figure 5. Particle size distributions of CLA emulsions stabilized by 0.67 wt% WPI, and 1.33 wt% GA and 2.0 wt% WPI/GA ISCs (r = 0.5) at pH 4.4.

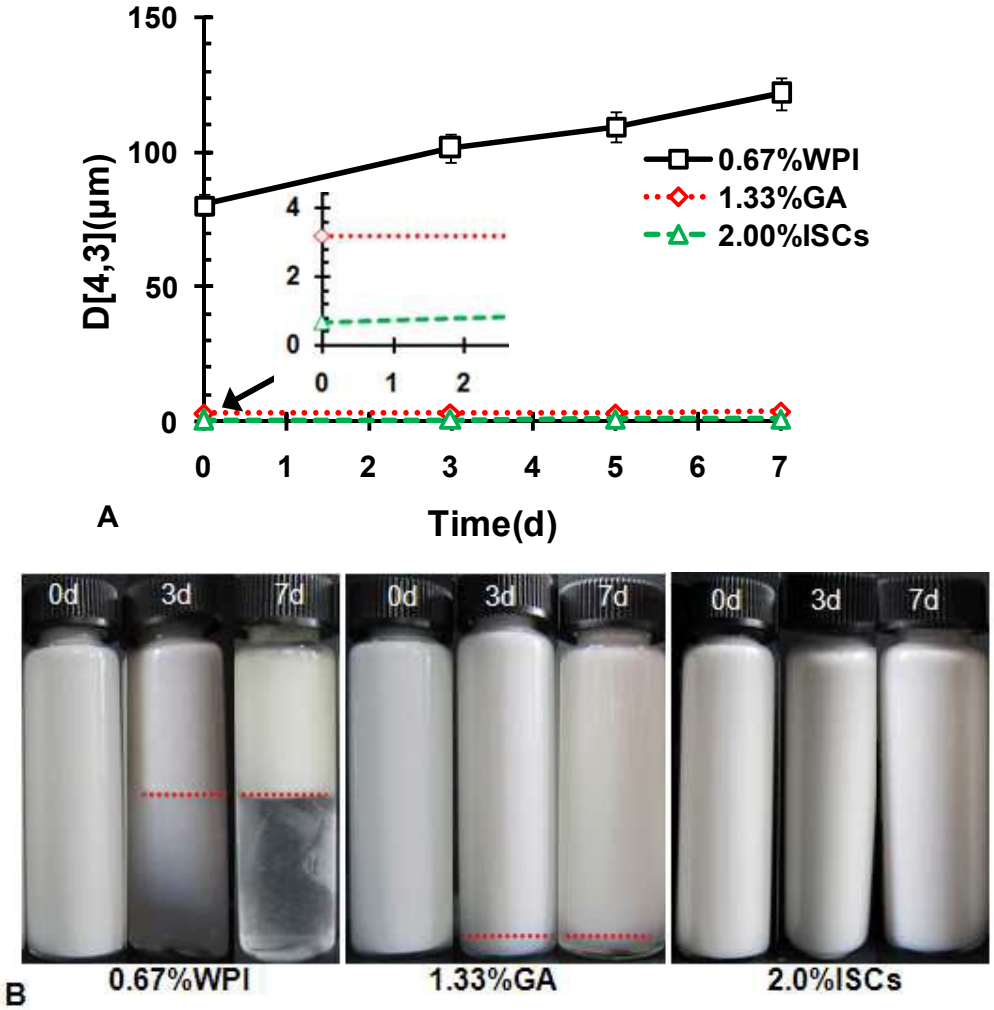

Figure 6. The plot of volume weighted mean diameter D[4,3] against storage time at 40 °C for CLA emulsions prepared with 0.67 wt% WPI, 1.33 wt% GA and 2.0 wt% WPI/GA ISCs, respectively (A), and the corresponding images of the emulsions taken at 0, 3 and 7 days of the storage (B).

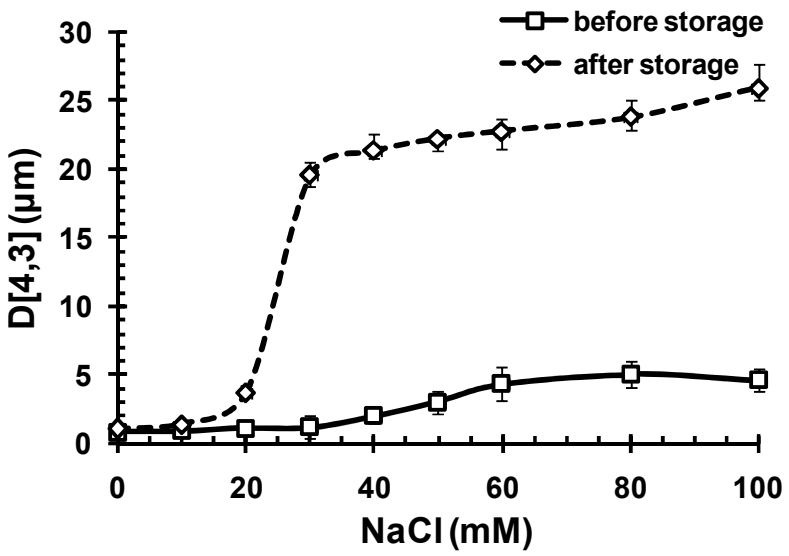

Figure 7. Plot of D[4,3] as a function of NaCl concentration before and after the storage at 40 °C for 7 days. The CLA emulsion was stabilized with 2.0 wt% WPI/GA ISCs (r = 0.5, pH=4.4).

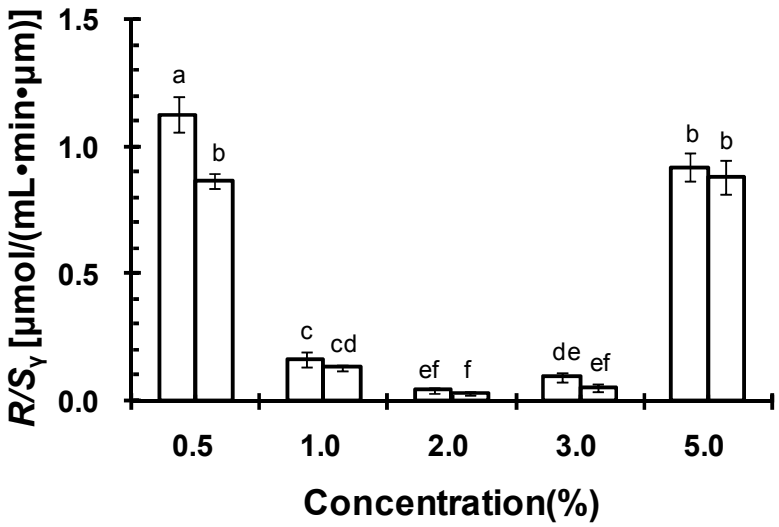

Figure 8. Normalized oxygen consumption rate R/S_v for CLA emulsions stabilized with various ISCs concentrations at 40 °C with (dot column) and without (blank column) exposure to light. Oxygen consumption rate (R) was calculated from the slopes of oxygen concentration-time curves. S_v stands for the specific surface area of CLA emulsions. Values of each column with different superscripts (a-f) are significantly different at $P < 0.05$.

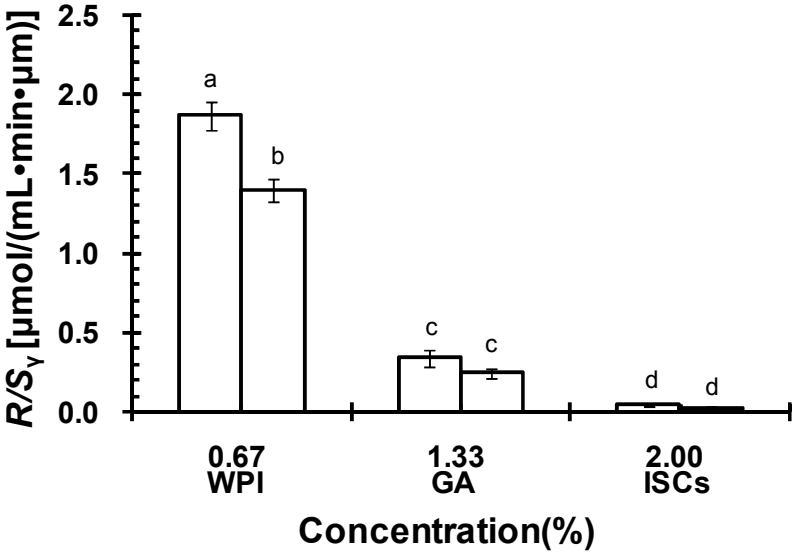

Figure 9. Normalized oxygen consumption rate R/S_v for CLA emulsions stabilized by WPI, GA, and ISCs respectively at 40 °C with (dot column) and without (blank column) exposure to light. Oxygen consumption rate (R) was calculated from the slopes of oxygen concentration-time curves. S_v stands for the specific surface area of CLA emulsions. Values of each column with different superscripts (a-d) are significantly different at $P < 0.05$.